



Supplementary Materials for

Return to quiescence of murine neural stem cells by degradation of a pro-activation protein

Noelia Urbán, Debbie van den Berg, Antoine Forget, Jimena Andersen, Jeroen A.
Demmers, Charles Hunt, Olivier Ayrault, François Guillemot
correspondence to: noelia.urban@crick.ac.uk or francois.guillemot@crick.ac.uk

This PDF file includes:

Materials and Methods
Figs. S1 to S14
Table S1
References 19 to 35

Materials and Methods

Animals:

Huwe1 is X-linked, so males are hemizygous for the Huwe1^{fl} or wild-type alleles (Huwe1^{fl/Y} or Huwe1^{+/Y}). We used males only for the study of Huwe1 function in the adult brain, and we have used the term Huwe1^{fl} to refer to the floxed allele for simplicity throughout the text. *GLAST-CreERT2* mice (11) were crossed with *Huwe1^{fl}* (7) and with *Rosa26-floxed-stop-YFP (RYFP)* reporter mice (19) to generate *GLAST-CreERT2^{CRE/+}; Huwe1^{fl/Y}; RYFP^{YFP/YFP}* and *GLAST-CreERT2^{CRE/+}; Huwe1^{+/Y}; RYFP^{YFP/YFP}*. Only males were used from the *Nestin-CreERT2* (20), *Ascl1-CreERT2* (21), *Z/EG* (stock 004178, The Jackson laboratory) and *Confetti* (22) mice for the clonal analysis experiments. Animal care was conducted in accordance with the guidelines of the Francis Crick Institute.

Tamoxifen and BrdU/EdU administration:

For activation of the CreERT2 recombinase, postnatal day 60 (P60) animals were administered intraperitoneally (ip) 2 mg (57-67mg/Kg) 4-hydroxytamoxifen (Sigma-Aldrich) once a day for 5 consecutive days. To examine proliferating progenitors, mice received a single ip injection of 2 mg bromodeoxyuridine (BrdU, Sigma-Aldrich, 10 mg/ml in PBS) 2 hours prior tissue collection. For the label retention experiments before tamoxifen, mice were administered BrdU in the drinking water (0.2 mg/ml) ad libitum for 5 days, followed by two days with normal water before tamoxifen administration. Alternatively, mice received three daily injections of 2 mg BrdU immediately followed by tamoxifen administration. For the label retention experiment a month after tamoxifen administration, mice received 5 daily BrdU injections followed by administration of BrdU in the drinking water (1 mg/ml) for 5 consecutive days and were sacrificed 20 to 22 days later. For the cell cycle exit assay, a single ip injection of 1mg of EdU (EdU, Santa Cruz Biotechnology, 10 mg/ml in PBS) was administered to the mice 24 hours before perfusion. For the analysis of *CcnD1* expression in cycling cells, EdU was administered in the drinking water (0.2 mg/ml) ad libitum for 48 hours before perfusion.

Tissue preparation and immunofluorescence:

Animals were perfused transcardially with phosphate buffered saline (PBS) for 3 min followed by 4% paraformaldehyde (PFA) in PBS for 12 min. Brains were post-fixed with 4% PFA during 2 hours at 4°C, washed with PBS and sectioned coronally at 40 µm using a vibratome (Leica). The immunofluorescence was performed as previously described (4) and the primary and secondary antibodies are listed in Table S1. For BrdU labeling, sections were labeled first with other primary antibodies (YFP, GFAP or S100β) and were afterwards fixed for 30 min with 4% PFA and washed 3 times with PBS. BrdU-unmasking was performed by treatment with pre-warmed 2N HCL for 30 min at 37°C, washed with 0.1M sodium tetraborate and processed for BrdU labeling. EdU was detected using Click-iT® EdU Imaging kit (Invitrogen).

Microscopic analysis and quantification:

Images were acquired using an SP5 confocal microscope (Leica). The whole section was imaged with a z-step of 1 µm for counting NSCs and picnotic nuclei or 2 µm for

counting other cell types. For total cell counts, labeled cells were counted in every sixth or twelfth 40 μm section through the entire rostrocaudal length of the DG. To present estimated total numbers per dentate gyrus, cells counted were divided by the thickness of the tissue imaged and then multiplied by the total length of the dentate gyrus, which was not significantly different between control and *Huwel*cKO mice at any age analyzed. To count NSCs, cells were deemed radial if the cell body clearly associated with a DAPI positive nucleus that was located in the subgranular zone and had a single GFAP+ radial process extending through at least two thirds of the granule layer unless stated otherwise. For quantification of percentage of cells expressing markers, at least 50 cells were counted per animal of a minimum of 4 animals per genotype. For quantification of the intensity of signal, at least 15 cells were selected per animal of a minimum of 4 animals per genotype. The intensity of the signal in the nucleus for the different channels was measured using ImageJ and selecting only the DAPI+ region of a single z plane of every selected cell. The intensity value was then normalized to the background levels of staining for each channel in each picture and expressed as a fold change with respect to the average value of neurons as a reference cell type.

Cell lines and cell culture

The embryonic NSC line was obtained from the ventral telencephalon of embryonic day 14 *Huwel*^{F1/Y} and *Huwel*^{F1/F1} mice. NS5 and embryonic NSCs were grown on laminin-coated dishes as described (23). For obtaining adult hippocampus-derived neural stem cells, 7 to 8 weeks old *Huwel*^{F1/Y} mice were sacrificed, the dentate gyrus was dissected (24) and cultures were obtained as previously described (25). Cultures were amplified as neurospheres for two passages and then transferred to adherent plates and cultured in standard adult hippocampal stem cell conditions (26).

Cell treatments, transfection and transduction:

For the calculation of the half-life of Ascl1 protein, 100 $\mu\text{g}/\text{ml}$ Cycloheximide (Sigma) was added to the media for the specified times shown and immediately lysed for protein preparation. To check the dependency on the proteasome of Ascl1 degradation, cells were cultured in 50mM (S)-MG132 (Cayman chemical) during 90 minutes and immediately lysed for protein preparation. Cells were lysed with Passive lysis buffer (Promega) supplemented with 20 μM Clasto-Lactacystin-b-lactone (Cayman chemical) and 1x Phosphatase inhibitor cocktail 2 (Roche). Transfections were performed with the nucleofector method (Amaxa), following manufacturer's instructions. Briefly, 5 to 7 μg of DNA were transfected per 5 million cells using the program A33 and the NSC specific kit. Transduction of CRE was performed with CMV-CRE adenovirus (vector biolabs) at a MOI of 100. CMV-null (i.e. empty) adenovirus were used as control at the same MOI. To generate inducible V5-tagged Ascl1-expressing NS cells the coding sequence of the V5 tag was inserted into lentiviral plasmid Tet-O-FUW-Ascl1 (kind gift from Marius Wernig, Addgene #27150 (27)). Lentiviral particles were produced by co-transfection with psPax2 and pMD2.G (kind gifts from Didier Trono, Addgene #12260 and #12259) in HEK293T cells and concentrated by ultracentrifugation. NS cells were simultaneously transduced with lentiviruses for V5-Ascl1 and rtTA (kind gift from Rudolf Jaenisch, Addgene #20342, (28)). Expression of V5-Ascl1 was induced for 6 hours by addition of 1 $\mu\text{g}/\text{ml}$ doxycycline (Sigma).

NIH-3T3 cells were infected with retroviruses encoding 8xHis-Ub, together with either non-targeting shRNA (sh-Ctrl) or Huwe1 shRNA (sh-Huwe1). NIH-3T3 cells were transfected with a pcDNA3-Ascl1-3xFlag-HA 24h after infection using lipofectamine 2000 (Invitrogen). 72 h after infection, the cells were treated with 10 μ M MG132 for 4 h and harvested. Ubiquitination assays were then performed as described in (29). Briefly, cell pellets were lysed in 8M urea buffer and His-ubiquitinated species were pulled down using His-select Nickel Affinity gel (Sigma). Eluates and total lysates were resolved by electrophoresis in 4-12% Bis-Tris NuPAGE gels (Invitrogen). The membranes were immunoblotted with an antibody against HA (Roche). Retroviruses were generated in HEK293T cells as previously described (29).

Protein purification and Mass Spectrometry:

Control and V5-Ascl1-expressing NS cells were expanded to 10 confluent 14 cm diameter dishes (2x10⁸ cells), scraped in ice cold PBS, nuclear extracts were prepared (30) and diluted to 100mM NaCl with C-0 (20mM Hepes pH7.6, 0.2mM EDTA, 1.5mM MgCl₂, 20% glycerol). Complete EDTA-free protease inhibitors (Roche) and 15 μ M MG132 (Sigma) were added to all buffers. 40 μ l of anti-V5 agarose beads (Sigma) were equilibrated in buffer C-100* (20mM Hepes pH7.6, 100mM KCl, 0.2mM EDTA, 1.5mM MgCl₂, 0.02% NP-40, 20% glycerol), blocked in 0.2mg/ml chicken egg albumin (Sigma), 0.1mg/ml insulin (Sigma) and 1% fish skin gelatin (Sigma) in C-100* and added to 1.5ml nuclear extract in no stick microtubes (Alpha Laboratories) for 3 hours at 4°C in the presence of 225 units Benzonase (Novagen). Beads were washed 5 times for 5 minutes with C-100* and boiled in 30 μ l SDS loading buffer. Eluted proteins separated by polyacrylamide gel electrophoresis were stained with Colloidal Coomassie (Invitrogen) and entire gel lanes were analyzed by mass spectrometry as previously described (31). For small scale immunoprecipitations 2.5 μ g of V5 antibody, 25 μ l of protein G dynabeads (Novex) and 200 μ l nuclear extract were used. Normal mouse IgG served as control and 25 units of Benzonase or 25 μ g/ml ethidium bromide were added where indicated.

FACS sorting, RNA isolation and quantitative real-time PCR:

The dentate gyrus from control and Huwe1cKO mice were dissected and YFP+ cells were sorted as previously described (4). RNA was reverse transcribed using the High Capacity cDNA Reverse Transcription Kit (Applied Biosystems) following manufacturer's instructions. Gene expression was detected using TaqMan Gene expression assays (Applied Biosystems) as described by the manufacturer and performed on a 7500 real time PCR system (Applied Biosystems). Data was analyzed using standard protocols to calculate relative expression with the ddCT method using Gapdh, ActinB and Ppia as endogenous controls and normalized to the expression of the control condition in each case. Each probe was analyzed in duplicates for at least 3 independent samples per group.

Statistical analyses:

Statistical analyses were conducted using a two-sample unpaired t test assuming Gaussian distribution with Welch's correction using Prism software. All graphs represent the mean \pm sem. Significance is stated as follows: p>0.05 (ns), p<0.05 (*), p<0.01 (**), p<0.001 (***)

Fig. S1.

Huwei1 interacts with Ascl1 in Neural Stem Cells.

(A) Table showing the Mascot and emPAI scores and the number of unique and total peptides for Ascl1-interacting proteins in embryonic stem cell-derived NSCs (NS5). E-proteins (TCF12/HEB, TCF4/ITF2 and TCF3/E2A) are known heterodimerization partners of Ascl1, and Ascl1 is shown as a control. See also the methods section for details on the mass spectrometry experiment. **(B)** Western blot analysis shows that V5-tagged Ascl1 expressed in NS5 cells co-immunoprecipitates endogenous Huwei1. The interaction is independent of DNA binding as it was not affected by the addition of Benzonase (Benzo) or Ethidium Bromide (EtBr).

A

Symbol	Accession	Mascot score	Empai	Uniq pept	Total pept	Description
Huwe1	A2AFQ0	3610	0.61	62	83	E3 ubiquitin-protein ligase HUWE1
Tcf12 (HEB)	Q61286	1800	4.55	25	72	Transcription factor 12
Tcf4 (ITF2)	Q60722	1575	7.73	23	88	Transcription factor E2-alpha
Tcf3 (E2A)	E9PVV2	1119	3.47	18	51	Transcription factor 3
Ascl1	Q7TNT5	374	1.71	5	27	Achaete-scute complex homolog 1

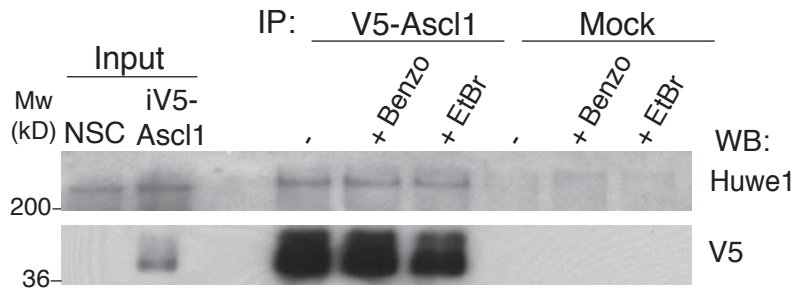
B

Figure S1 Urbán et al.

Fig. S2

Huwei1 promotes the degradation of Ascl1 in embryonic telencephalon-derived and adult hippocampus-derived NSCs.

(A-E) NSCs were derived from the ventral telencephalon of *Huwei1^{f/f}* embryos of embryonic day 14.5. (A) Western blot analysis with a HECT domain-specific antibody (32) of two control NSC cultures transduced with control adenovirus and two cultures transduced with CRE-expressing adenovirus shows that the HECT domain of Huwei1 was efficiently excised. This deletion does not affect the microRNAs hosted by the *Huwei1* gene. (B) Expression of Ascl1 protein was strongly increased upon *Huwei1* inactivation in cultured NSCs. Arrows point to Ascl1+ nuclei. (C) Western blot analysis of the expression of Huwei1 substrates Cdc6, Hdac2 and Mcl1 and E-proteins E47 and E12 (E2A), which stabilise Ascl1 through formation of heterodimers (33). *Huwei1* inactivation does not affect the expression of these proteins in NSCs. Beta actin (Actb) was used as a loading control. Other substrates of Huwei1 including N-myc (V-Myc Avian Myelocytomatosis Viral Oncogene Neuroblastoma Derived Homolog), MyoD (Myogenic Differentiation 1) and Atoh1 (Atonal BHLH Transcription Factor 1) are not expressed in NSCs (our own observations). (D) Ascl1 is destabilized in a proteasomal-dependent manner. Treatment with proteasome inhibitor MG132 for 90 minutes increased the amount of Ascl1 protein in NSCs. Triangles represent loading of 1, ½ and ¼ doses of protein lysate. Actin and Hdac2 are used as a loading control. (E) Representative western blot used for the analysis of Ascl1 half-life in Fig. 1C. (F-G) Neural stem cells cultures were derived from dissected adult dentate gyrus (see methods). Immunolabeling showed that Huwei1 is co-expressed with Ascl1 in cultured adult hippocampus-derived neural stem cells (F). Note the nuclear and cytoplasmic subcellular localization of Huwei1 protein. Expression of Ascl1 protein was strongly increased upon *Huwei1* inactivation in cultured NSCs (G). Ascl1mRNA was not changed (see Fig. S14 C). Arrows point to Ascl1+ nuclei.

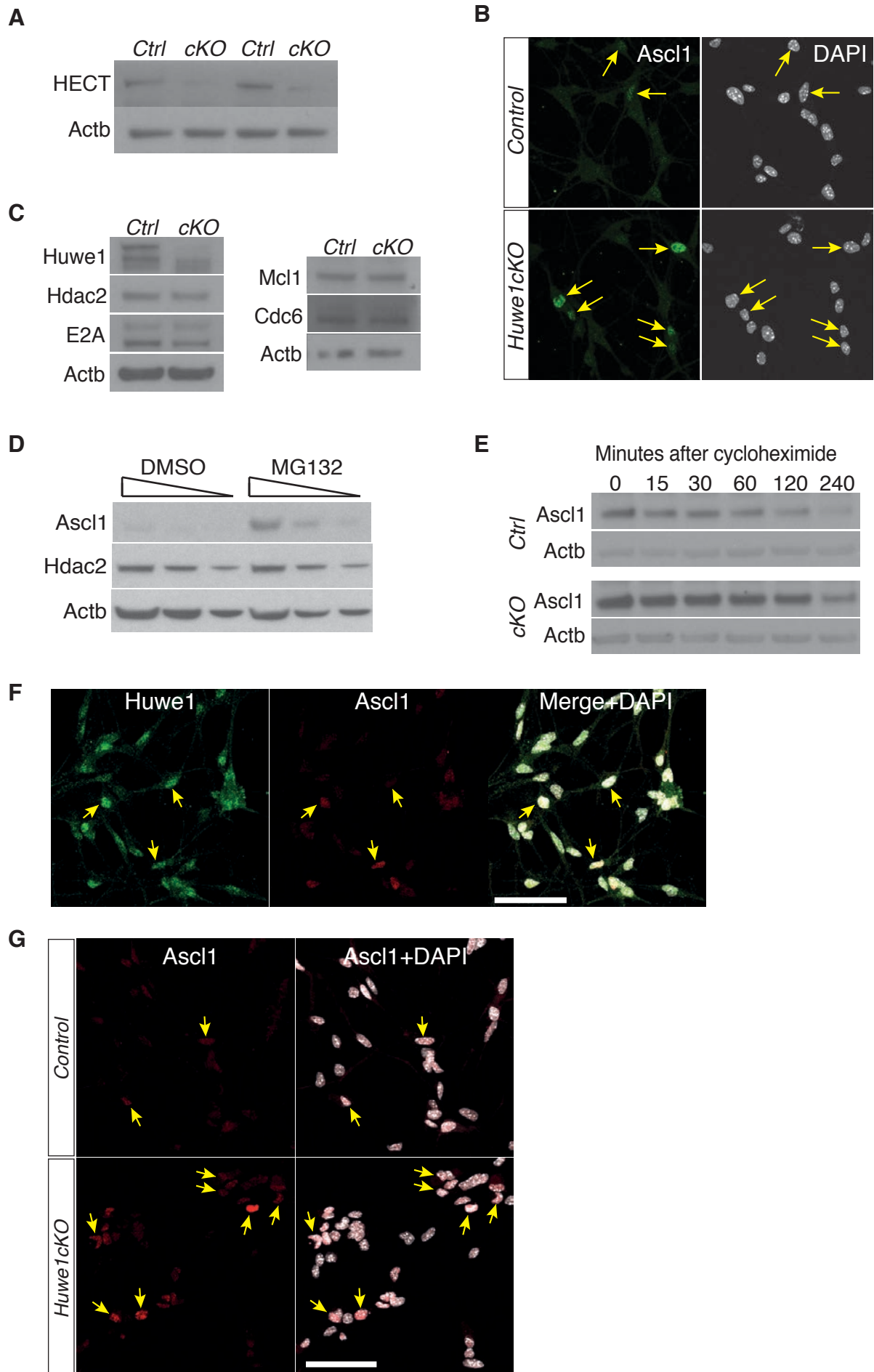


Figure S2 Urbán et al.

Fig. S3

Huwei1 is expressed in adult neural stem cells and their progeny in the dentate gyrus.

(A) Immunohistochemistry showing that Huwei1 is expressed in the dentate gyrus. While Huwei1 is nuclear in some neuronal populations (see CA3 in the image), it is both nuclear and cytoplasmic in the dentate gyrus and appears diffuse. Scale bar, 300 μm . **(B)** Western Blot for Huwei1 was performed in dissected tissue from the cortex (CTX), subventricular zone (SVZ) and dentate gyrus (DG). Huwei1 is highly expressed in the DG and CTX and less so in the SVZ. **(C)** Huwei1 is expressed in Sox2+ cells in the subgranular zone of the DG. The arrowhead in C points to a Sox2+, Huwei1 high cell while the small arrow points to a Sox2+, Huwei1 low cell. Scale bar, 20 μm . **(D)** Since transcription factors are ubiquitinated and degraded by the proteasome in the nucleus (34), we examined the nuclear content of Huwei1 in several cell types of the subgranular zone. Huwei1 levels are lower in stem and progenitor cells (Sox2+) and in proliferating intermediate progenitors (Ki67+) than in neuroblasts (DCX+) and neurons (NeuN+). The intensity of Huwei1 immunolabeling is normalized to the average level in neurons (=1). N = 49 (Sox2), 21 (Ki67) and 54 (DCX and NeuN) cells from 3 control mice. All graphs represent the mean \pm sem.

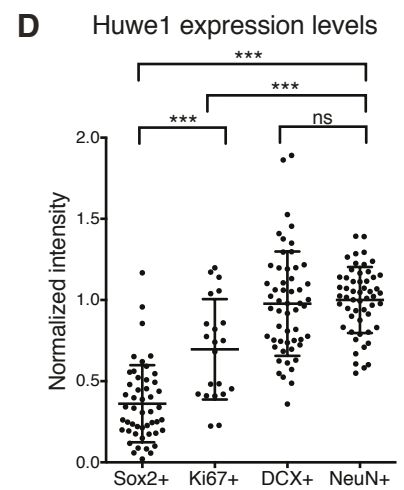
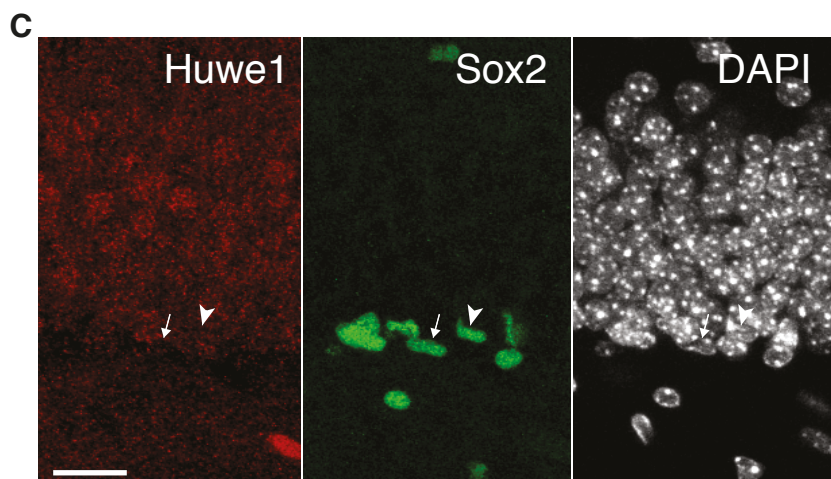
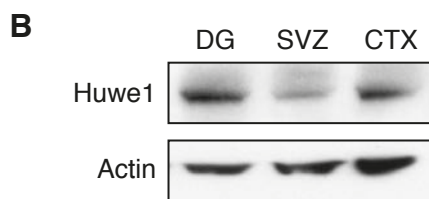
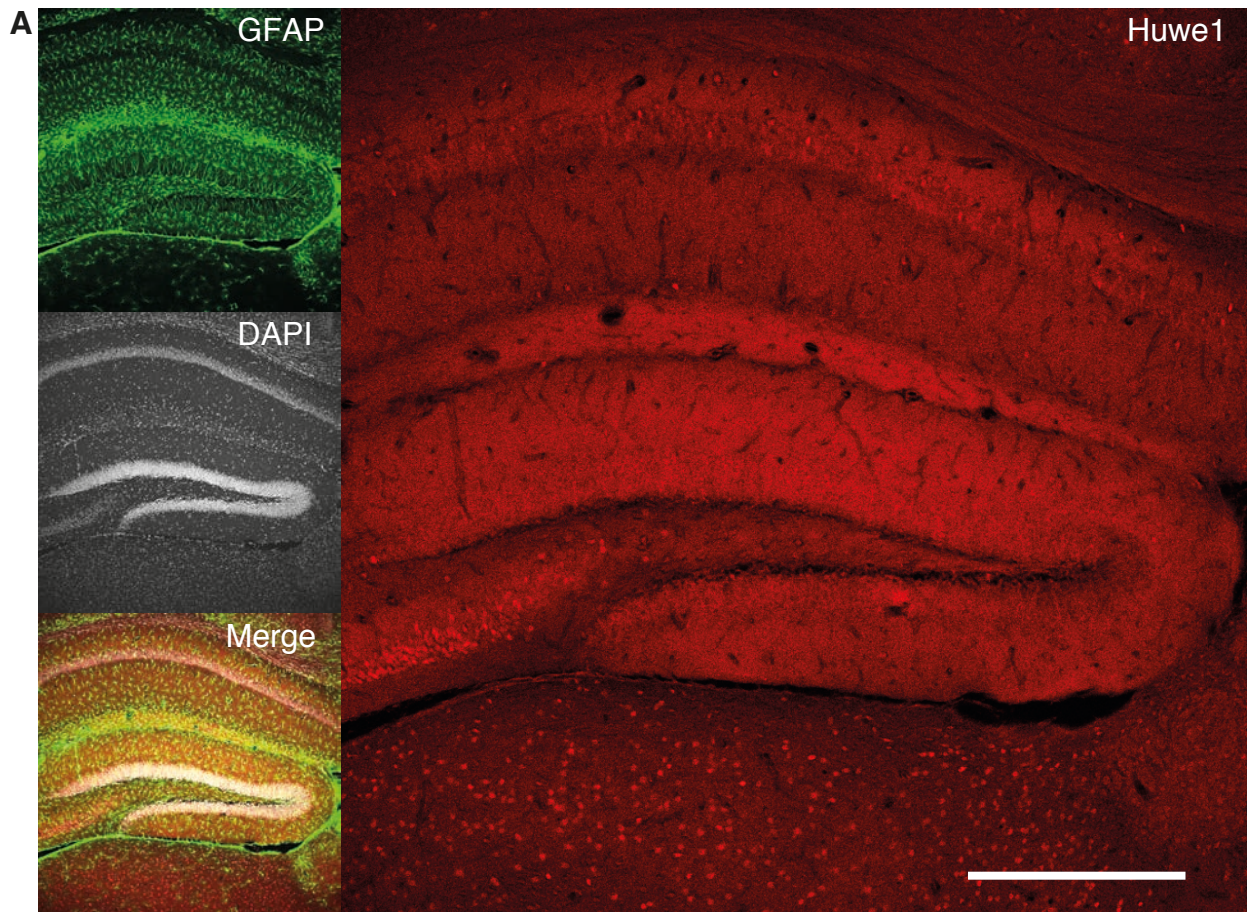


Figure S3 Urbán et al.

Fig. S4

Inactivation of *Huvel* *in vivo* increases expression of *Ascl1* in the subgranular zone.

(A) Tamoxifen injections at P60 efficiently eliminate *Huvel* from the stem cell lineage at P90. Floxed *Huvel* is less stable than wild-type *Huvel* (32) and therefore the level of *Huvel* protein is lower in recombined cells (YFP+ encircled cells, yellow arrows) in *Huvel**CKO* mice than in control mice. **(B)** The number of *Ascl1*+ cells in the subgranular zone is greatly increased upon inactivation of *Huvel* at P90. Yellow arrows point to *Ascl1*+ nuclei. Scale bars, 20 μ m.

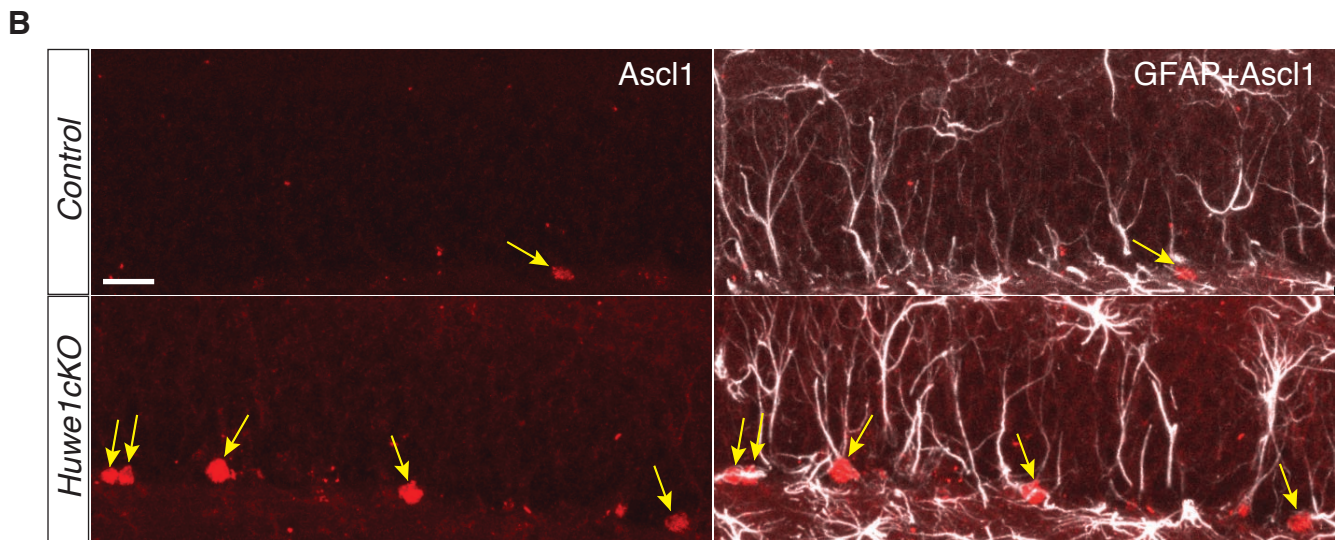
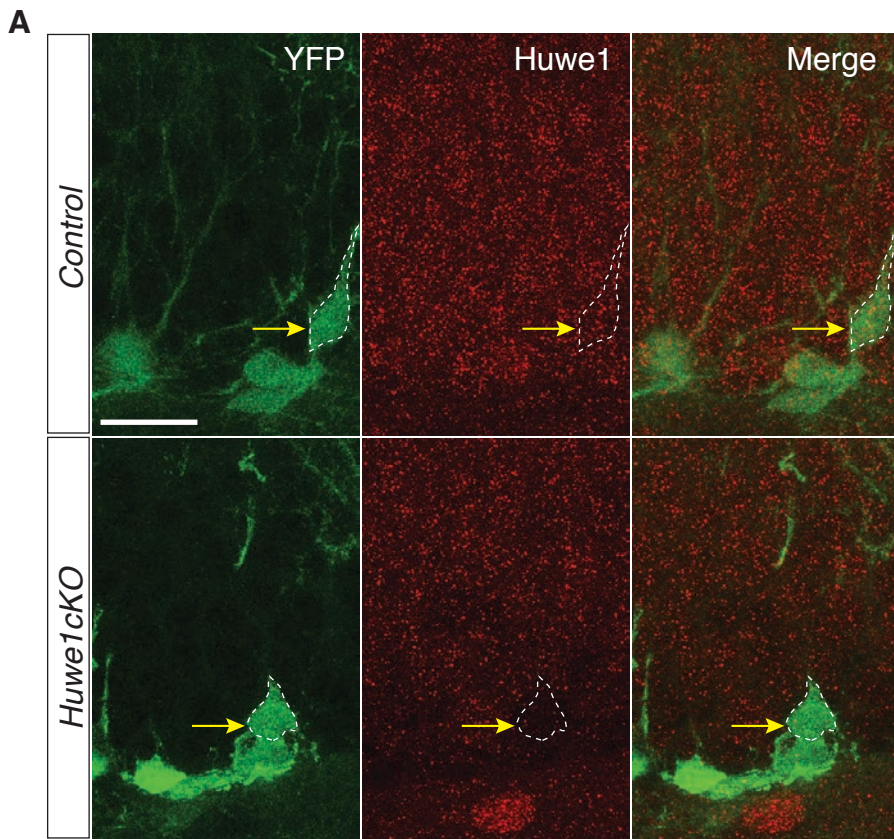


Figure S4 Urbán et al.

Fig. S5

Inactivation of *Huwe1* *in vivo* does not change the expression of other known *Huwe1* substrates.

(A to C) The expression of *Huwe1* substrates N-myc (A), Hdac2 (B) and Mcl1 (C) is not changed in *Huwe1**CKO* mice 30 days after tamoxifen administration. Yellow arrows point to NSCs. Scale bars, 20 μ m.

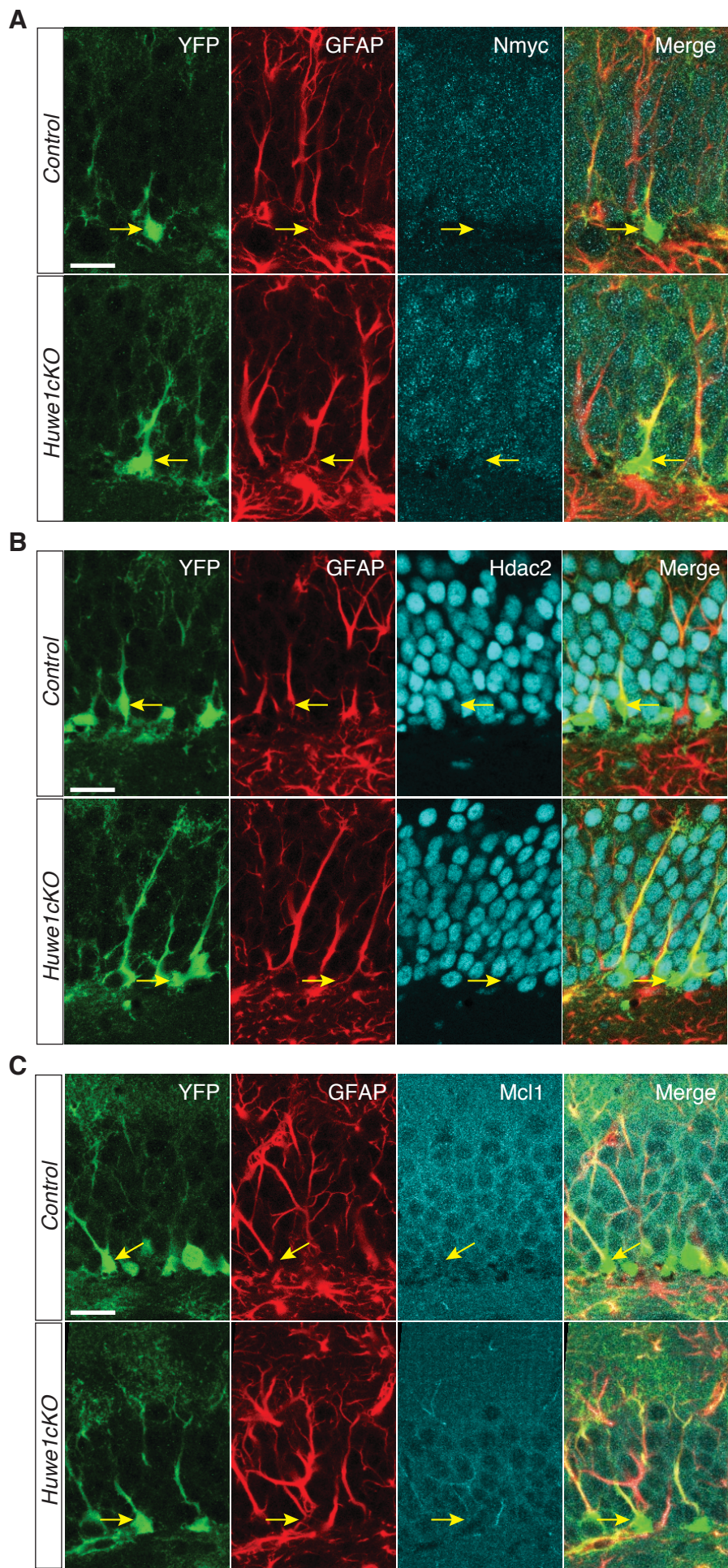


Figure S5 Urbán et al.

Fig. S6

Inactivation of *Huvel* *in vivo* results in up-regulation of *Ascl1* in intermediate progenitors and neuroblasts.

(A) Tamoxifen was administered at P60 and analysis was performed one month later at P90. (B) The total number of stem cells is not significantly changed in *HuvelcKO* mice compared to control mice. (C-F) *Ascl1* expression is maintained in a higher percentage of intermediate progenitors and neuroblasts in *HuvelcKO* mice than in control mice, as shown by co-localization of *Tbr2* and *Ascl1* (C, E) and of *DCX* and *Ascl1* (E). The total number of proliferating (*Ki67*⁺) cells remained unchanged (F). The image in (D) is a representative image of the counting in Figure 2C. Yellow arrows in C point to *Tbr2*⁺ cells. N = 3 mice per condition. (G-I) No new neuroblasts (*DCX*⁺ *YFP*⁺) are generated in the dentate gyrus of *HuvelcKO* mice 3 months after *Huvel* inactivation. N = 3 mice per condition. All graphs represent the mean \pm sem. Scale bars, 20 μ m.

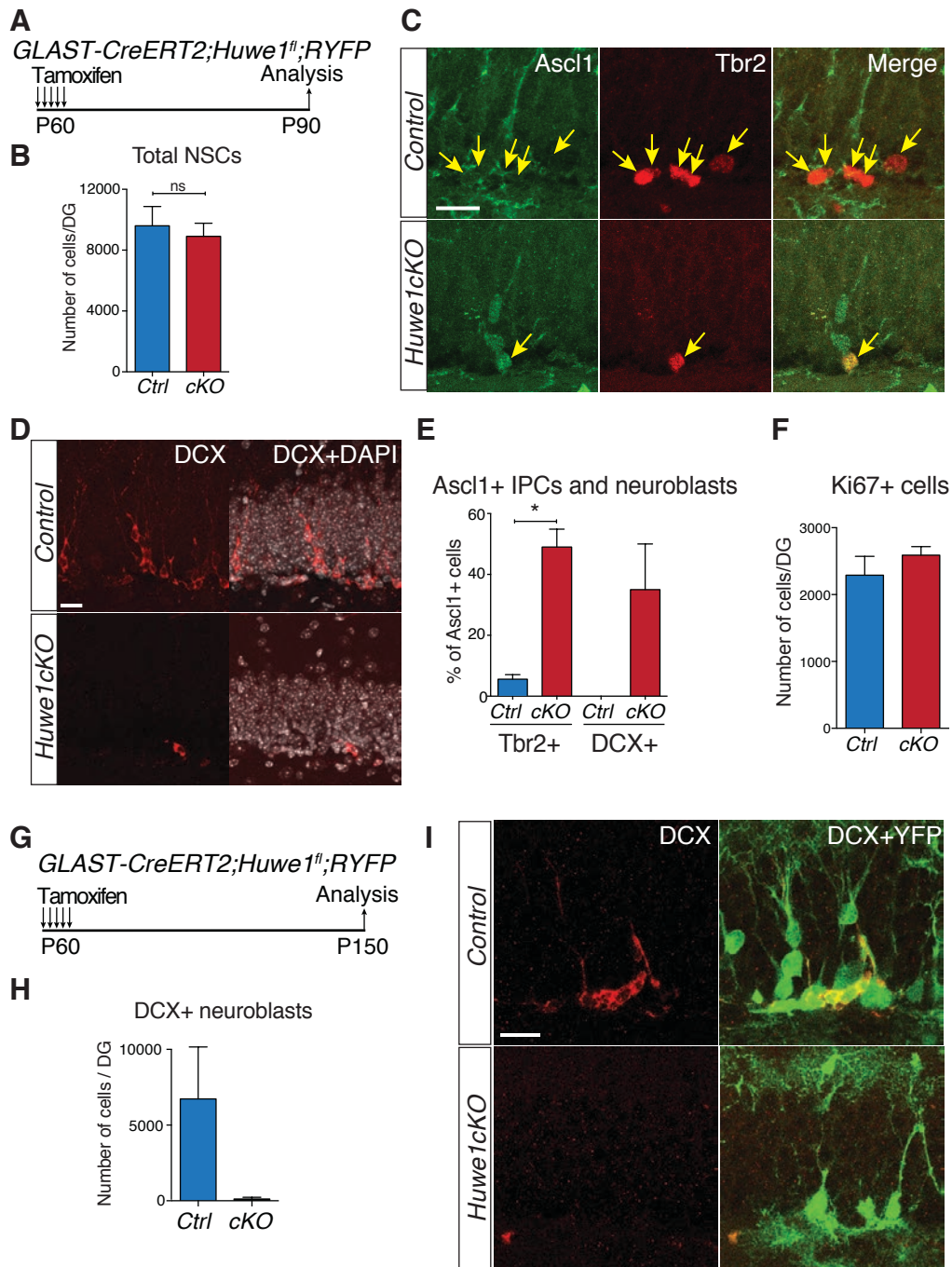


Figure S6 Urbán et al.

Fig. S7

***Huvel* inactivation does not induce a switch to gliogenesis in the dentate gyrus.**

(A) NG2+YFP+ oligodendrocyte precursors are not found in *HuvelcKO* or control mice at P90. **(B and C)** The number of astrocytes (S100 β +YFP+ in the subgranular zone) is similar in control and *HuvelcKO* mice on month after *Huvel* deletion. Yellow arrowheads point to S100 β -negative NSCs. N = 3 (control) and 4 (*HuvelcKO*) mice. The graph represents the mean \pm sem. Scale bars, 50 μ m.

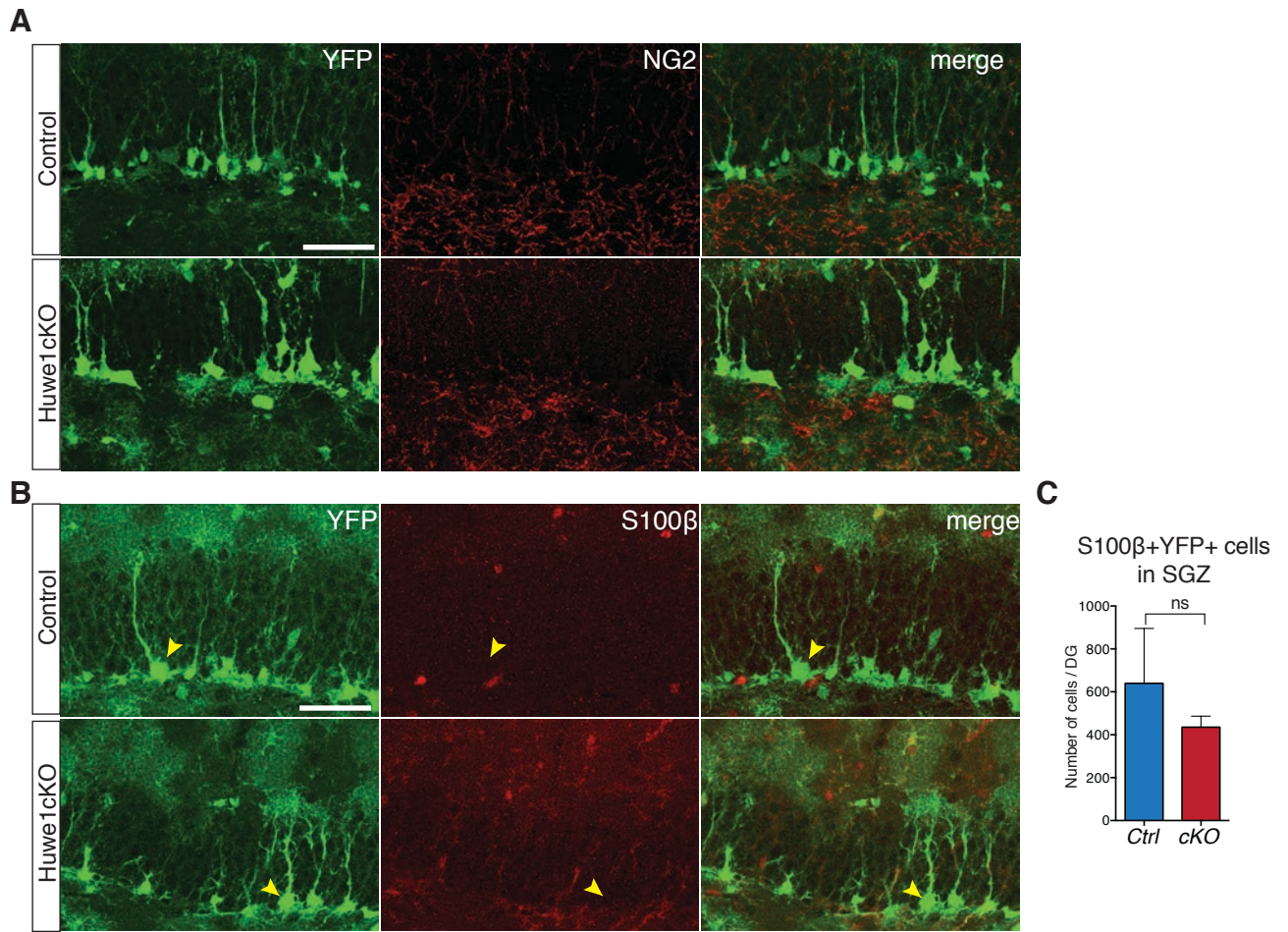


Figure S7 Urbán et al.

Fig. S8

***Huvel* inactivation increases cell death in the dentate gyrus.**

(A-C) One month after tamoxifen administration, the number of activated Caspase3+ cells is slightly higher, but not significantly, in *HuvelcKO* mice than in control mice. The number of picnotic nuclei is similar in *HuvelcKO* and control mice. Similarly, the density of Iba1+ cells in the subgranular zone is slightly increased, but not significantly, in *HuvelcKO* mice (E). N = 3 mice per condition in B and 4 (control) and 5 (*HuvelcKO*) mice in C. **(D-F)** In control mice, the population of dying cells is formed by intermediate progenitors and neuroblasts but only early intermediate progenitors are present in *HuvelcKO* mice. We therefore counted picnotic nuclei shortly after recombination to increase the proportion of intermediate progenitors among recombined cells. The difference between *HuvelcKO* and control mice is not significant but shows a clear trend towards a higher number of picnotic cells in *Huvel* mutants. The image in F shows microglia processes (Iba1+) engulfing picnotic nuclei in the subgranular zone of the DG. N = 3 mice per condition. Scale bar, 20 μ m. **(G and H)** Quantification of picnotic nuclei in proliferating progenitors one month after *Huvel* inactivation. We counted EdU+ picnotic nuclei in mice exposed to EdU in the drinking water for 48 hours before analysis. We observed a higher number of EdU+ picnotic cells in *HuvelcKO* mice. Note that at this time overall proliferation is similar in *HuvelcKO* and control mice (Fig. S6 F). N = 4 (control) and 6 (*HuvelcKO*) mice. **(I and J)** Quantification of the total number of YFP+ cells at different time points after recombination shows that recombined cells are eliminated in *HuvelcKO* mice. N = 3 mice per condition. All graphs represent the mean \pm sem.

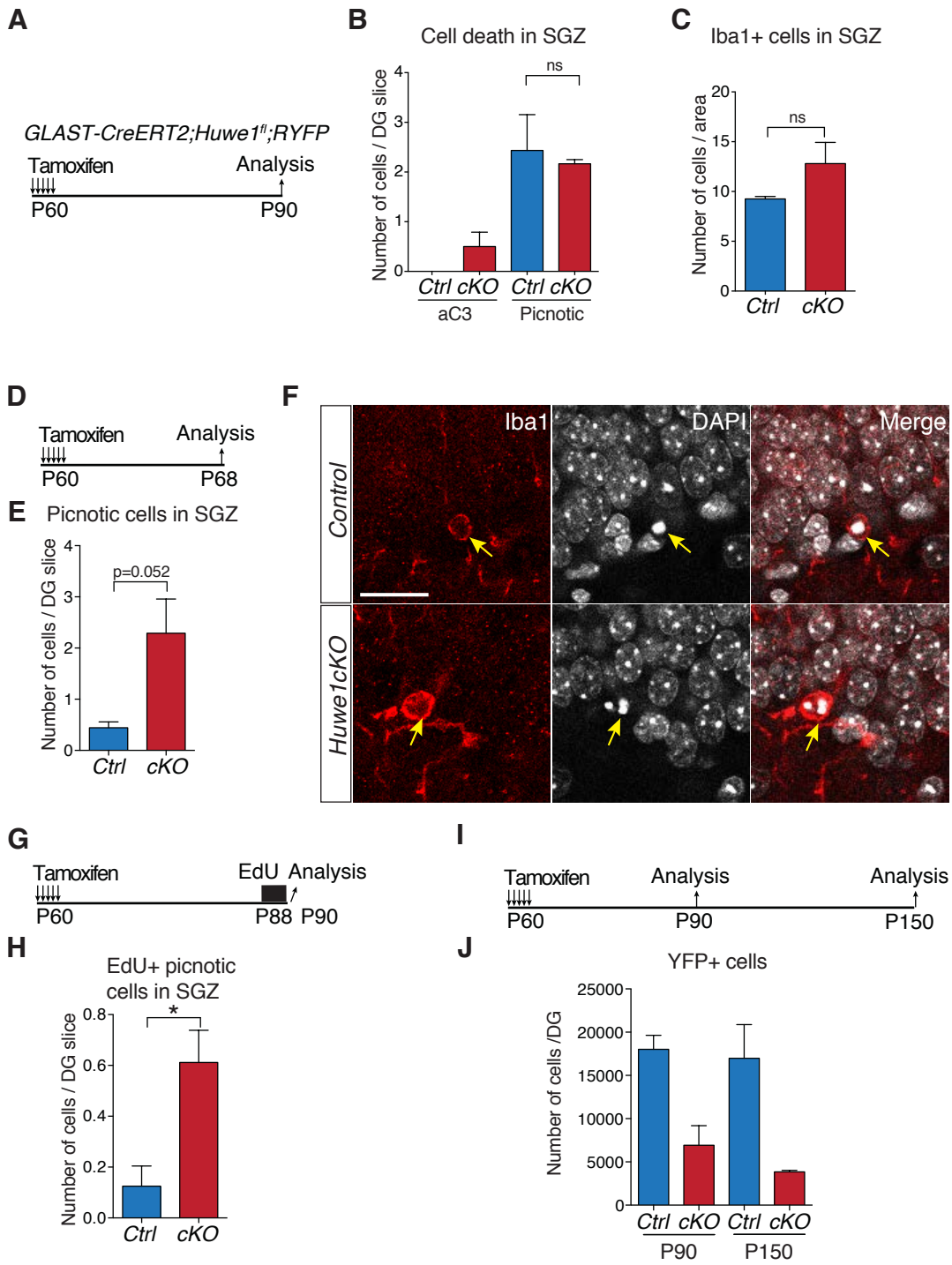


Figure S8 Urbán et al.

Fig. S9

Adult hippocampal stem cells fail to return to quiescence in *HuwelcKO* mice.

(A-C) Hippocampal stem cells do not exit quiescence prematurely in *HuwelcKO* mice. BrdU was added to the drinking water of P60 mice for 5 days, followed two days later by *Huwel* inactivation and induction of YFP expression in NSCs. Analysis was performed three weeks after the last tamoxifen injection (A). The total number of BrdU-retaining YFP+ cells (Fig. 3B) and the total number of BrdU-positive cells in the subgranular zone remained similar in *HuwelcKO* and control mice. Yellow arrows point to BrdU-positive NSCs. N = 3 (control) and 6 (*HuwelcKO*) mice. **(D to F)** An additional BrdU retention experiment (consisting of 3 consecutive daily injections of BrdU followed immediately by tamoxifen administration) shows no difference in the number of BrdU-retaining YFP+ NSCs, further demonstrating that *Huwel* inactivation does not affect already quiescent NSCs. The total number of BrdU+ cells was also not changed between *HuwelcKO* and control mice. N = 5 mice per condition. **(G to J)** The return to quiescence of hippocampal stem cells is impaired in *HuwelcKO* mice. *Huwel* was inactivated at P60, BrdU was administered at P90 and analysis was performed three weeks later. BrdU-retaining NSCs (identified by position and morphology) do not express the astrocytic and type- β NSC marker (35) S100 β (H, 0 S100 β + out of 49 BrdU-retaining NSCs). We found no S100 β +YFP+ BrdU-retaining astrocytes in the subgranular zone of granule cell layer at this stage. *Huwel* inactivation in NSCs resulted in BrdU dilution and reduced numbers of BrdU-positive NSCs (Fig. 3H) and total BrdU-positive cells (J) in *HuwelcKO* mice compared with controls. Yellow arrows point to NSCs. N = 5 (control) and 3 (*HuwelcKO*) mice for batch 1 (shown), and 2 (control) and 3 (*HuwelcKO*) mice for batch 2. Scale bars, 20 μ m. All graphs represent the mean \pm sem.

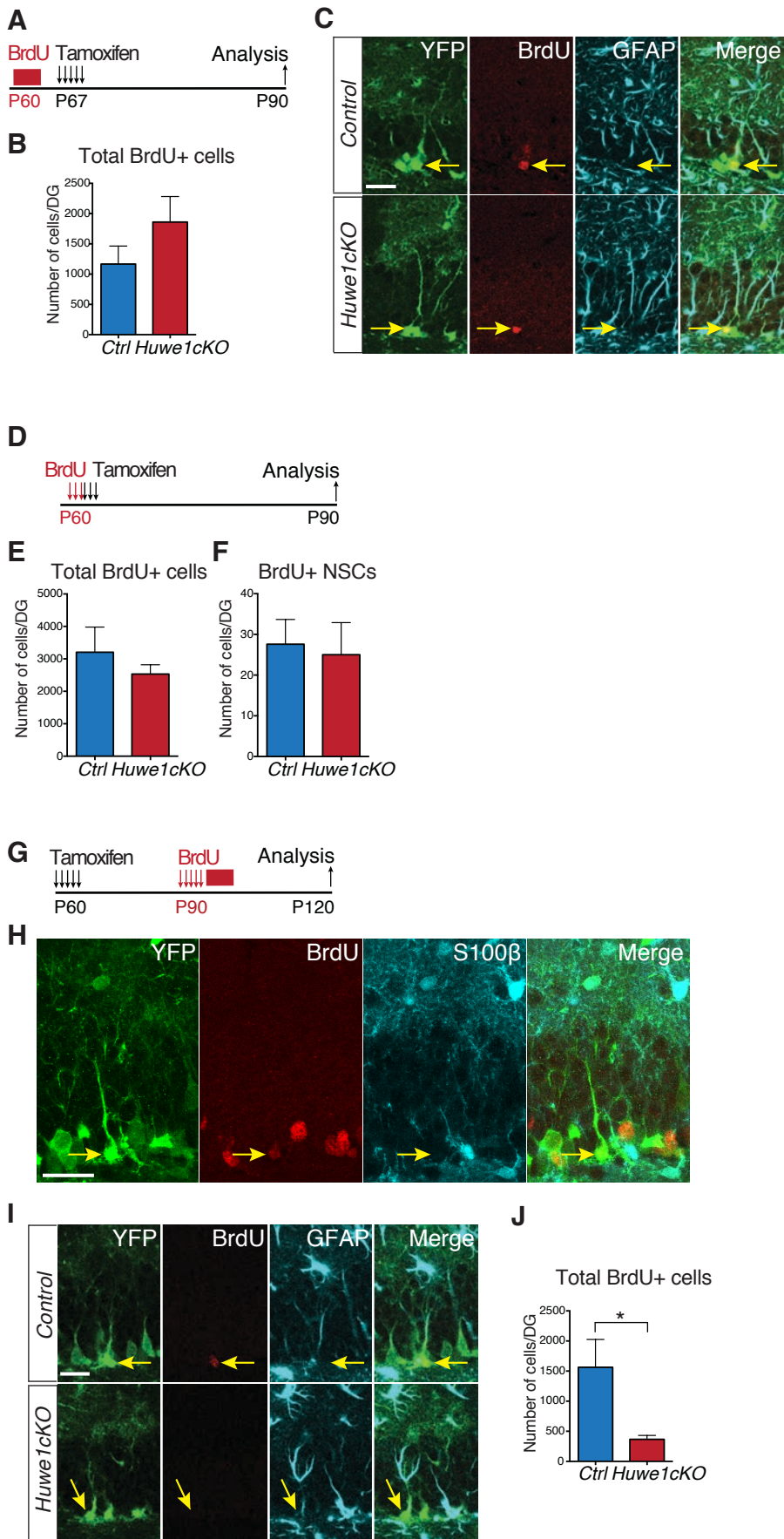


Figure S9 Urbán et al.

Fig. S10

Clonal analysis cannot be performed in *Huwe1cKO* mice.

(A) List of the different genotypes and tamoxifen dosages used to attempt clonal labeling of *Huwe1cKO* NSCs in the DG, and outcome of the recombination of the different reporter genes and the *Huwe1* gene. The doses of tamoxifen required to activate the three CreERT deleter transgenes tested (*GLAST-CreERT* (11), *Nestin-CreERT* (20) and *Ascl1-CreERT* (21)) and to recombine the three reporter transgenes tested (*Rosa-stop-YFP* (19), *Z/EG* (stock 004178, The Jackson laboratory) and *Confetti* (22)) in a few NSCs failed to delete the *Huwe1^{f/f}* gene. (B-D) As a representative example, *Glast-CreERT2; Huwe1^{f/f}; RYFP* mice yielded a relatively sparse labeling one month after administration of a low dose of tamoxifen (0.5mg). However, recombined cells in *Huwe1cKO* mice yielded the same number of intermediate precursors (IPCs) and neuroblasts as control mice. The image in D shows widespread co-localization of DCX and YFP in the *Huwe1cKO* DG. Arrows point to a double DCX-YFP-positive cell. N = 2 (*control*) and 3 (*Huwe1cKO*) mice. Scale bars, 100 μ m in the upper panel and 20 μ m in the lower panels. The graph represents the mean \pm sem.

A

Deleter	Reporter	Tam. Dose	Tam Conc.	Viability	Reporter Recombination	Huwe1FI recombination
NestinCREert2	Confetti	0.5mg	14-17 mg/Kg	Very Good	None	Very low/none
NestinCREert2	Confetti	2mg	57-67 mg/Kg	Good	Very sparse	Very low
NestinCREert2	RYFP	0.5mg	14-17 mg/Kg	Very Good	Very sparse	Very low/none
NestinCREert2	Z/EG	2mg	57-67 mg/Kg	Good	None	n.d
NestinCREert2	Z/EG	0.5mg	14-17 mg/Kg	Very Good	None	n.d
GlastCREert2	Confetti	2mg	57-67 mg/Kg	Good	Sparse	Medium/Low
GlastCREert2	RYFP	2mg	57-67 mg/Kg	Good	Very good	Medium/Low
GlastCREert2	RYFP	0.5mg	14-17 mg/Kg	Very Good	Sparse	Very Low/none
Ascl1CREert2	RYFP	2mg	57-67 mg/Kg	Good	Sparse	Very Low/none
Ascl1CREert2	RYFP	4mg	114-134 mg/Kg	Poor	Sparse	Very low

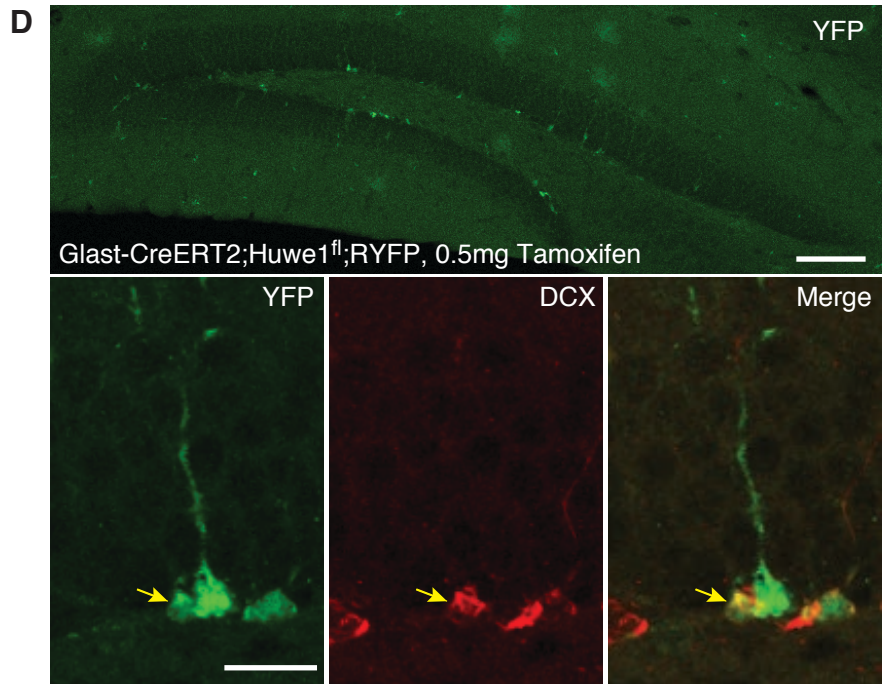
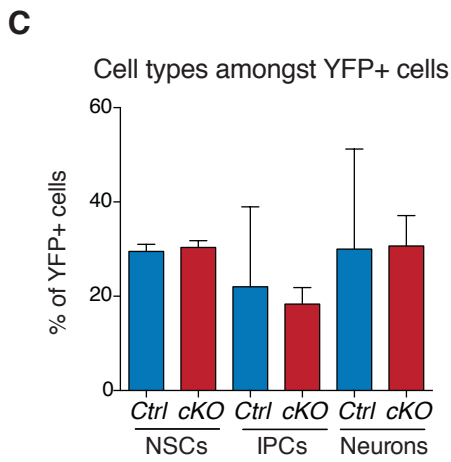
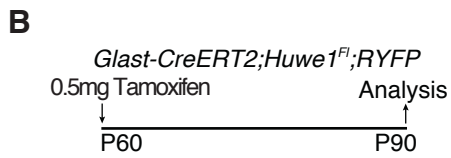


Figure S10 Urbán et al.

Fig. S11

***Huwe1cKO* NSCs do not exit the cell cycle and do not become astrocytes.**

(A-B) At the time of analysis of cell cycle exit (P68), *Huwe1cKO* mice already have a significantly higher number of *Ascl1*⁺ cells per dentate gyrus than control mice (A). N = 3 (control) and 4 (*Huwe1cKO*) mice. **(C-E)** The graph in D represents the same data as Fig. 3F. N = 5 (control) and 6 (*Huwe1cKO*) mice. No EdU⁺ NSCs converted into astrocytes (S100 β ⁺) after a 24 hour pulse of EdU. N = 22 EdU+Ki67⁻ NSCs from 5 control mice. Yellow arrows point to an EdU-positive Ki67-negative S100 β -negative NSC **(F to I)** Control and *Huwe1cKO* mice presented low and comparable numbers of S100 β ⁺ astrocytes and Type β NSCs in the granular cell layer (GCL) and the subgranular zone (SGZ) of the dentate gyrus. Yellow arrowheads point to S100 β -negative NSCs. N = 5 (control) and 6 (*Huwe1cKO*) mice. Scale bars, 20 μ m. All graphs represent the mean \pm sem.

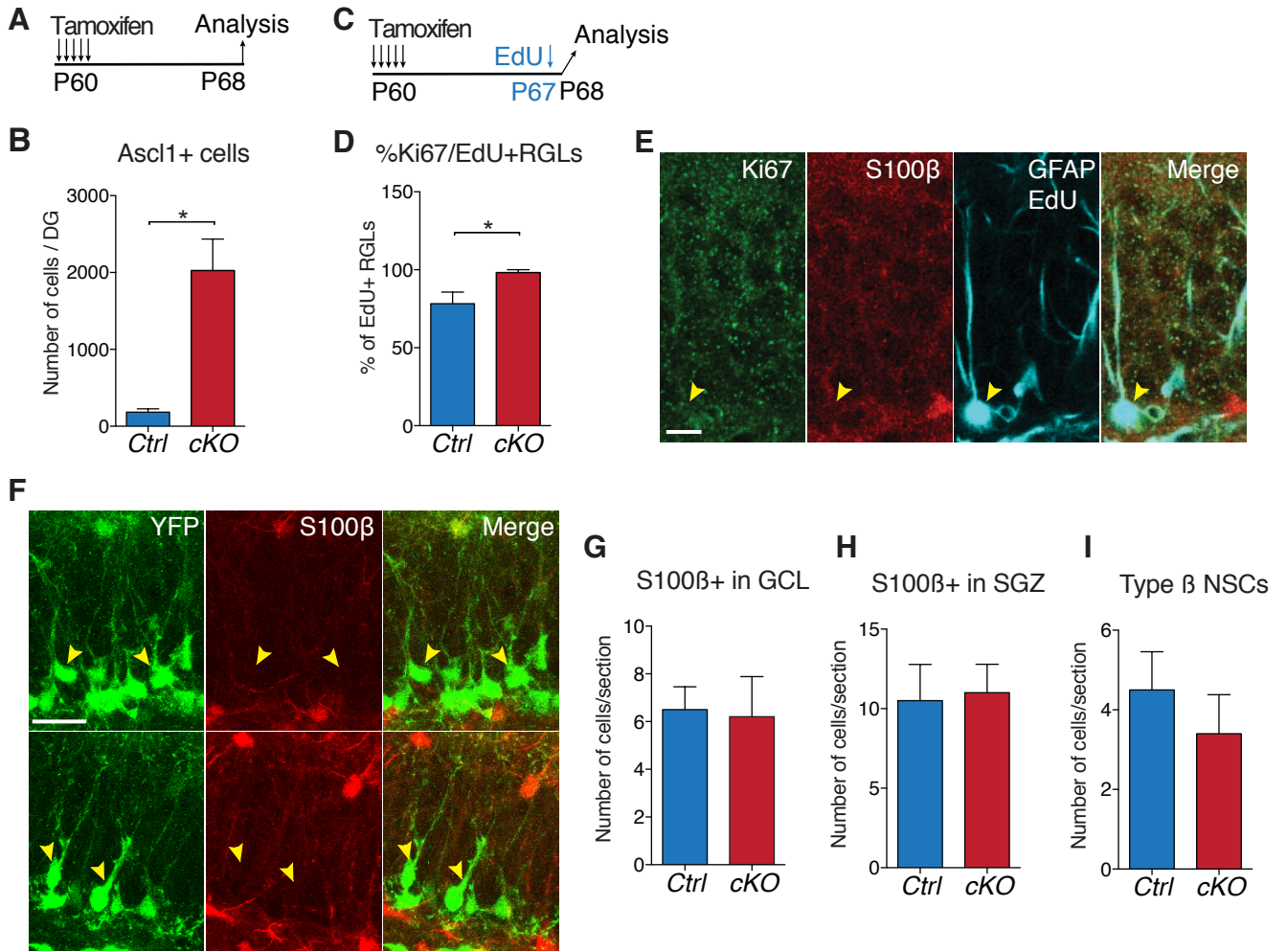


Figure S11 Urbán et al.

Fig. S12

Model of the distribution of hippocampal neural stem cells in distinct pools in young (P90) and older (P210) mice in control and *Huwe1cKO* mice.

We propose that in control mice, most proliferating hippocampal stem cells originate from a transient pool of quiescent stem cells (Resting pool), which is formed by cells that were once active and later exited the cell cycle. Stem cells that did not proliferate earlier (Dormant pool) also exit quiescence and enter the Active pool, but in smaller numbers. A fraction of dividing cells in the Active pool re-enter quiescence and replenish the Resting pool but most continue to divide and are eventually consumed. The three pools therefore become gradually and proportionally depleted at later times (P210).

In *Huwe1cKO* mice, proliferating hippocampal stem cells are not able to return to quiescence. Shortly after *Huwe1* inactivation (P90), the excessive proliferation of active stem cells leads to an enlargement of the Active pool and to a lack of replenishment of the Resting pool. At later time points (P210), the Resting pool becomes exhausted and as it is normally the main source of active stem cells, the size of the Active pool becomes severely reduced.

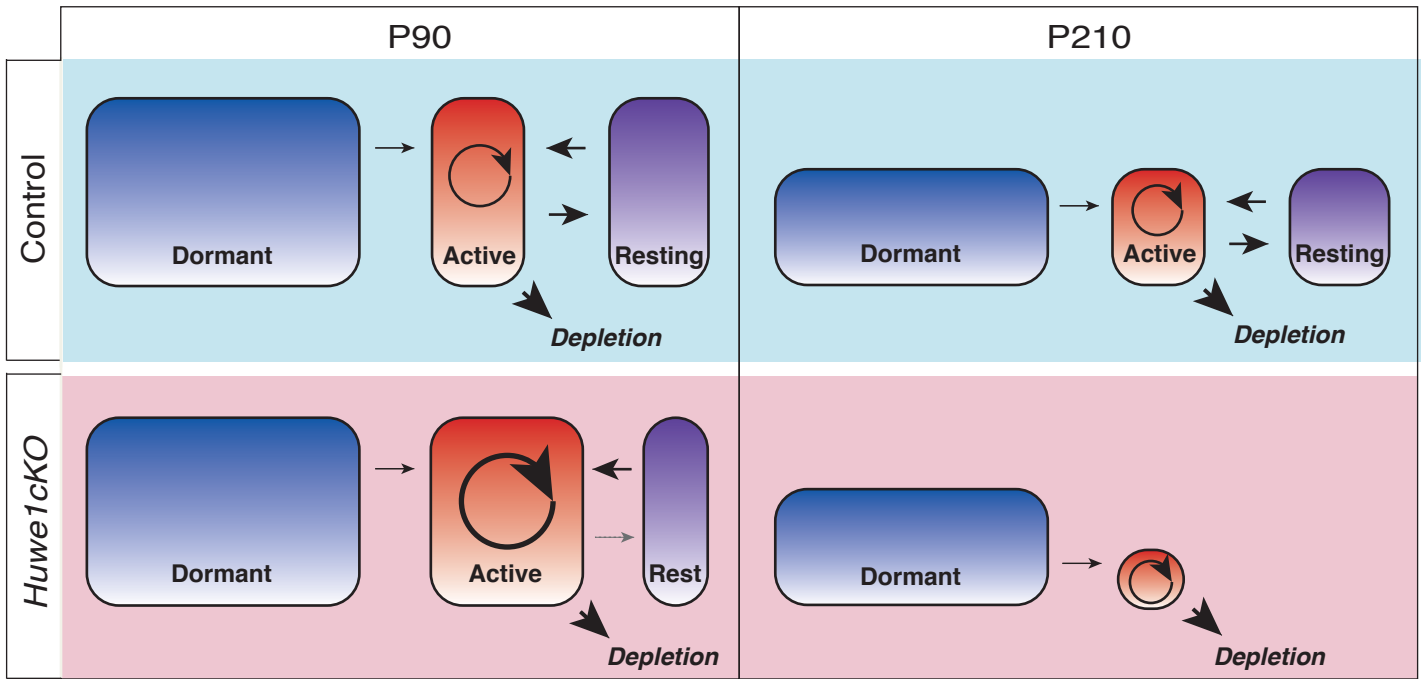


Figure S12 Urbán et al.

Fig. S13

***CcnD* genes are upregulated in *Huvel*-mutant NSCs in an *Ascl1*-dependent and cell cycle-independent manner.**

(A) The expression of *Ascl1* target genes, including cell cycle-related genes, *Rgs16* and *Dll1* (4, 14) and that of various cyclins and cyclin-dependent kinases was analyzed by qRT-PCR in *HuvelcKO* and control cultured embryonic telencephalon-derived NSCs. Both *CcnD1* and *CcnD2* are upregulated in *HuvelcKO* NSCs. For each condition, the results are normalized to the averaged expression of three housekeeping genes (*ActinB*, *Gapdh* and *Ppia*) and expressed as a fold change in *HuvelcKO* cells compared to control cells. **(B and C)** The number of *CcnD1*-positive but not of *Ki67*-positive cells is increased in *HuvelcKO* compared to *control* NSCs. N = 3 independent experiments. Scale bar, 50 μ m. **(D)** Inactivation of *Huvel* in cultured NSCs results in an increase in the expression of *CcnD1* and *CcnD2* that is rescued by *Ascl1* knockdown. *Huvel^{f/f}* NSCs were transduced with control or CRE adenovirus and transfected with control or *Ascl1* shRNA and analyzed by qRT-PCR. N = 3 experiments per condition. All graphs represent the mean \pm sem.

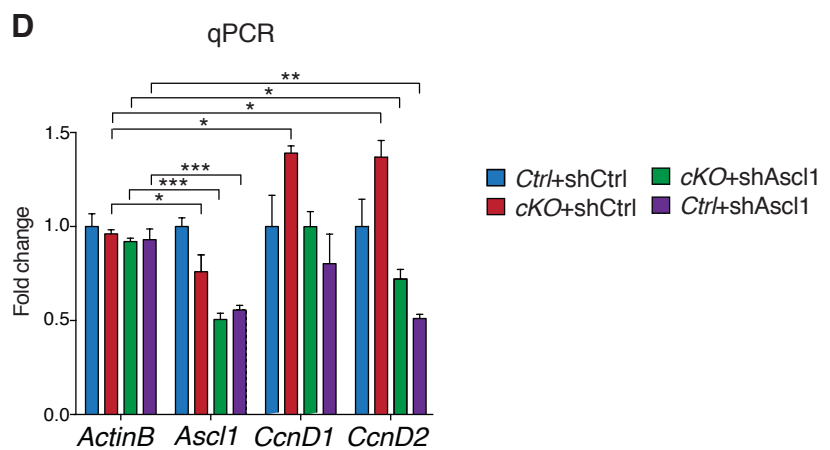
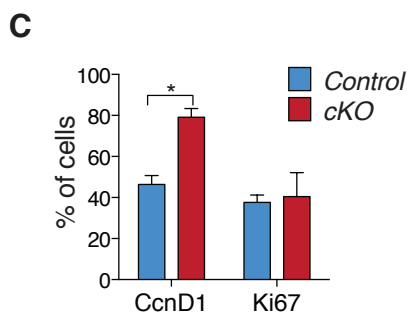
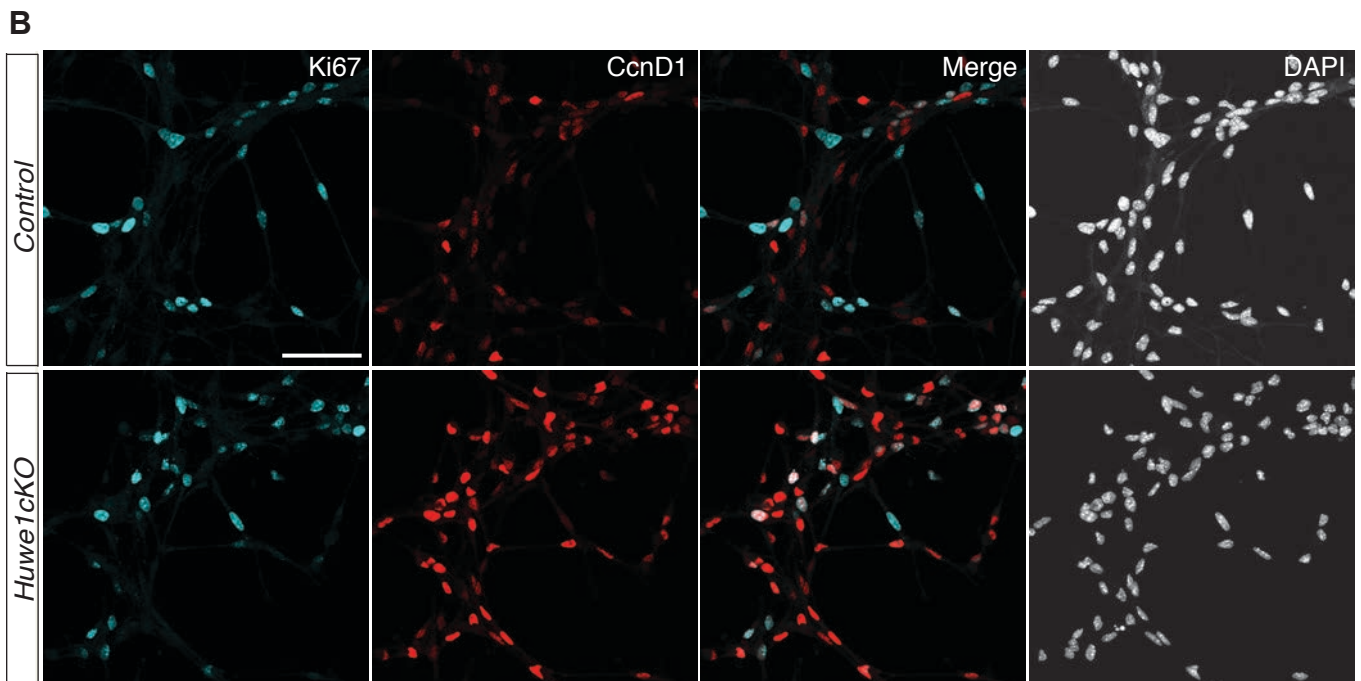
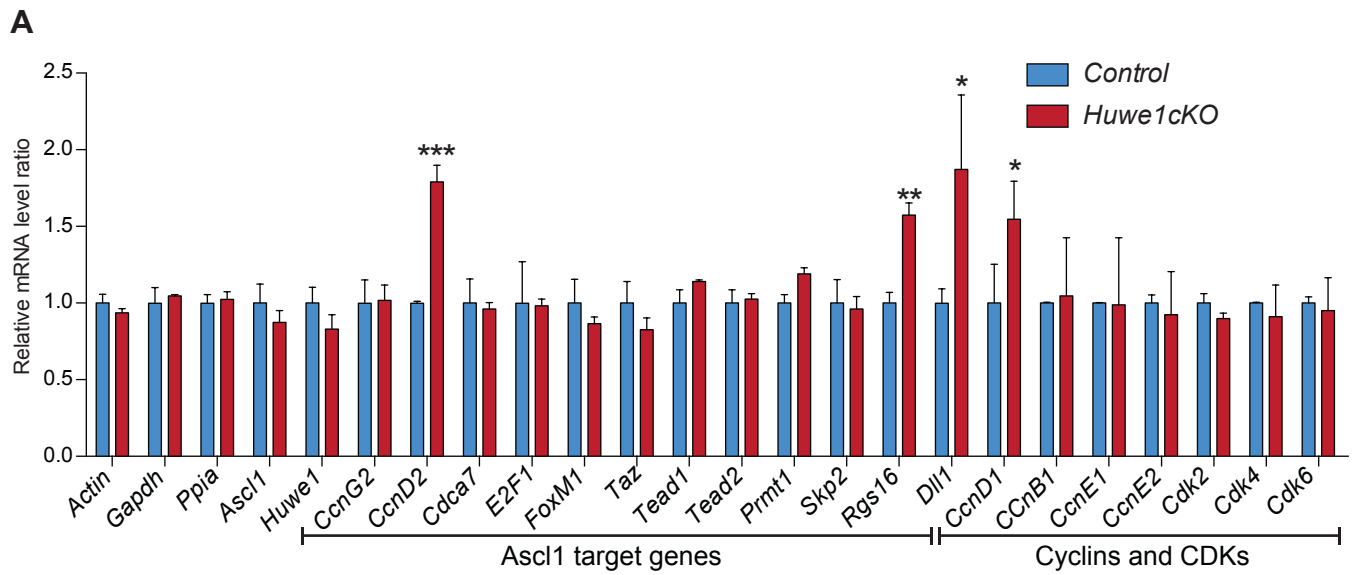


Figure S13 Urbán et al.

Fig. S14

***CcnD* genes are upregulated by loss of *Huvel* in adult hippocampal NSCs.**

(A) The number of *CcnD1*⁺ hippocampal NSCs is increased one month after *Huvel* inactivation, while *Ascl1* deletion abolishes *CcnD1* NSC expression in both *Huvel* mutant and control backgrounds. N = 3 mice per condition. **(B)** YFP⁺ cells from the dentate gyrus of control or *Huvel**CKO* mice were FAC-sorted and analyzed by qRT-PCR. Both *CcnD1* and *CcnD2* mRNA levels are increased in *Huvel**CKO* stem cells. The results are normalized to the averaged expression of two housekeeping genes (*ActinB* and *Gapdh*) and expressed as a fold change in *Huvel**CKO* compared to control cells. **(C)** The expression of *CcnD1* and *CcnD2* is increased in *Huvel**CKO* cultured adult hippocampal stem cells (AHSCs). For each condition, the results are normalized to the averaged expression of three housekeeping genes (*ActinB*, *Gapdh* and *Ppia*) and expressed as a fold change in *Huvel**CKO* cells compared to control cells. **(D to F)** EdU was added to the drinking water for 48 hours prior to the analysis. The number of EdU-positive hippocampal NSCs is increased one month after *Huvel* inactivation (E) and a higher percentage of EdU⁺ NSCs express *CcnD1* (F). The graph in F represents the same data as Fig. 4E. N = 6 mice per condition. All graphs represent the mean ± sem.

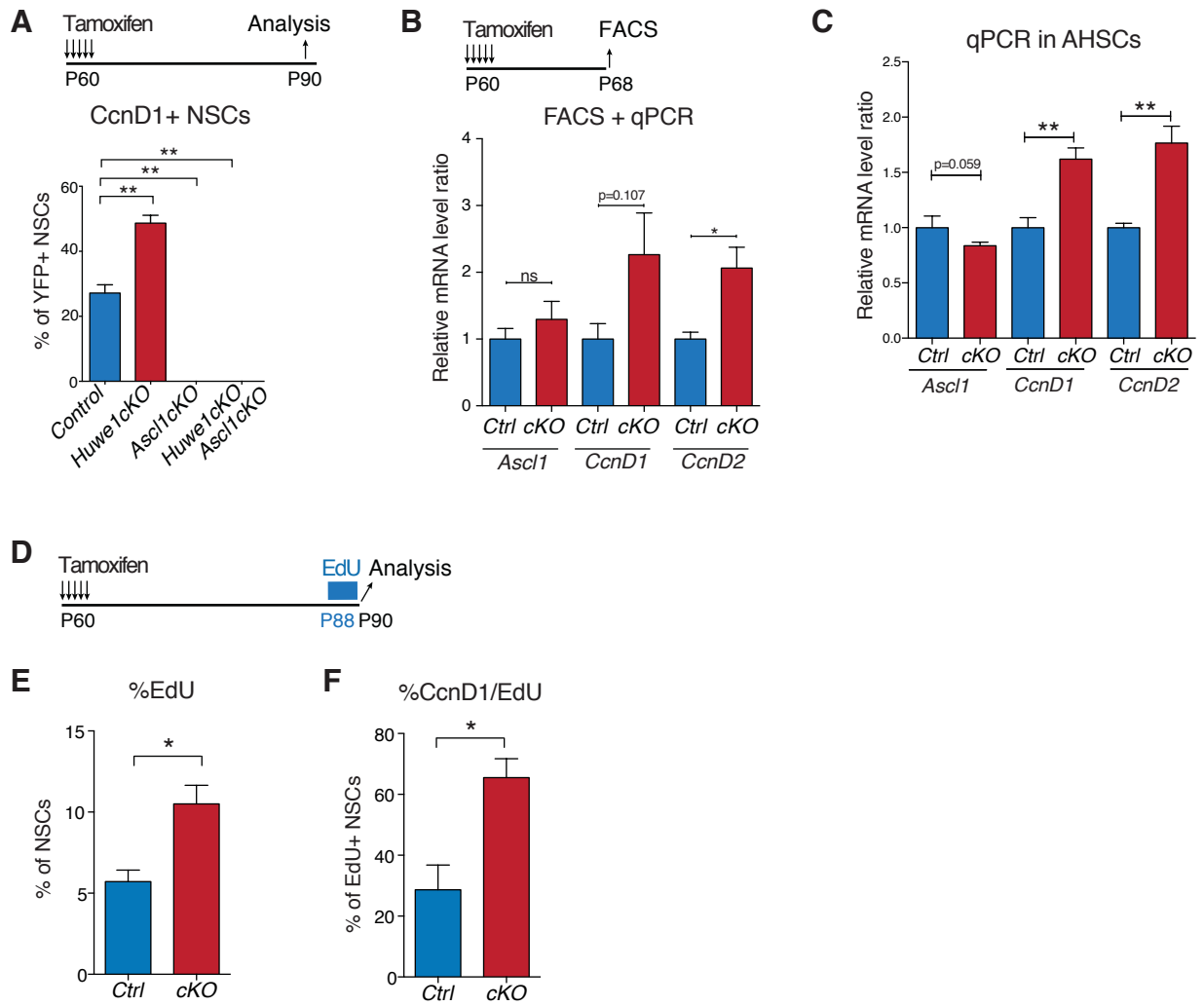


Figure S14 Urbán et al.

Table S1

List of primary and secondary antibodies used for Western Blot (WB) and immunohistochemistry (IHC).

Target Molecule	Species	Procedure	Dilution	Company (Catalog number)
Ascl1	mouse	WB	1:500	BD Pharmingen (556604)
Ascl1	mouse	IHC	1:100	BD Pharmingen (556604)
GFP	rabbit	IHC	1:1000	Invitrogen (A11122)
GFP	chicken	IHC	1:5000	Abcam (ab13970)
GFP	rat	IHC	1:1000	Nacalai Tesque (04404-84)
GFAP	rat	IHC	1:500	Invitrogen (13-0300)
GFAP	mouse	IHC	1:500	SIGMA (G6171)
BrdU	rat	IHC	1:1000	ABD Serotec (OBT0030CX)
Tbr2	rabbit	IHC	1:200	Abcam (ab23345)
DCX	goat	IHC	1:50	Santa Cruz Biotechnology (sc-8066)
Ki67	mouse	IHC	1:100	BD Biosciences (550609)
Ki67	rabbit	IHC	1:200	Leica/Novocastra (NCL-Ki67p)
CcnD1	rabbit	IHC	1:400	ThermoScientific (RM-9104)
Huwe1	rabbit	WB	1:1000	Bethyl Laboratories (A300-486A)
Huwe1	rabbit	IHC	1:200	Bethyl Laboratories (A300-486A)
Huwe1 (HECT)	rabbit	WB	1:500	LifeSpan Biosciences (LS-B1359)
Hdac2	mouse	WB	1:1000	Cell Signalling (5113)
Hdac2	mouse	IHC	1:500	Cell Signalling (5113)
E2A (E12 and E47)	rabbit	WB	1:500	Santa Cruz Biotechnology (sc-763)
Actb	rabbit	WB	1:1000	SIGMA (A2066)
Mcl1	mouse	WB	1:500	Abcam (ab31948)
Mcl1	rabbit	IHC	1:100	GeneTex (GTX102026)
Cdc6	mouse	WB	1:200	Santa Cruz Biotechnology (sc-13136)
Sox2	goat	IHC	1:500	Neuromics (GT15098)
NeuN	mouse	IHC	1:1000	Chemicon (MAB377)
Nmyc	mouse	IHC	1:200	Calbiochem (OP13L)
NG2	rabbit	IHC	1:200	Millipore (AB5320)
S100B	mouse	IHC	1:1000	SIGMA (S2657)
S100B	rabbit	IHC	1:200	Dako (Z0311)
cleaved caspase 3	rabbit	IHC	1:500	BD Pharmingen (559565)
Iba1	goat	IHC	1:500	Abcam (ab5076)
rat IgG	donkey	IHC-488	1:1000	Life Technologies (A21208)
rabbit IgG	donkey	IHC-488	1:1000	Life Technologies (A21206)
chicken IgG	donkey	IHC-488	1:1000	Jackson (703-545-155)
rat IgG	donkey	IHC-cy3	1:1000	Jackson (712-166-153)
rabbit IgG	donkey	IHC-cy3	1:1000	Jackson (711-166-152)
mouse IgG	donkey	IHC-cy3	1:1000	Jackson (715-166-151)
goat IgG	donkey	IHC-cy3	1:1000	Jackson (705-166-147)
rat IgG	donkey	IHC-647	1:1000	Jackson (112-175-167)
rabbit IgG	donkey	IHC-647	1:1000	Jackson (711-606-152)
mouse IgG	donkey	IHC-647	1:1000	Jackson (715-606-151)
goat IgG	donkey	IHC-647	1:1000	Jackson (705-605-147)
mouse IgG	rabbit	WB-HRP	1:1000	Dako (P0161)
rabbit IgG	goat	WB-HRP	1:1000	Dako (P0448)

Table S1 Urbán et al.